JHR 87: 291–308 (2021)
doi: 10.3897/jhr.87.72838
https://jhr.pensoft.net

RESEARCH ARTICLE

JOURNAL OF Hymenoptera RESEARCH
A peer-reviewed open-access journal
The International Society of Hymenopterists

Stink bug egg parasitoids (Hymenoptera, Scelionidae) associated with pistachio in Iran and description of a new species: *Trissolcus darreh* Talamas

Fateme Ranjbar[1], M. Amin Jalali[1], Mahdi Ziaaddini[1], Zahra Gholamalizade[1], Elijah J. Talamas[2]

1 *Department of Crop Protection, College of Agriculture, Vali-e-Asr University of Rafsanjan, Rafsanjan 7713936417, Iran* **2** *Division of Plant Industry, Florida Department of Agriculture and Consumer Services, Gainesville, FL, USA*

Corresponding author: Elijah J. Talamas (elijah.talamas@fdacs.gov)

Academic editor: Zachary Lahey | Received 10 August 2021 | Accepted 7 October 2021 | Published 23 December 2021

http://zoobank.org/E825C33D-4D0A-4B76-AAB0-6A7880850EDA

Citation: Ranjbar F, Jalali MA, Ziaaddini M, Gholamalizade Z, Talamas EJ (2021) Stink bug egg parasitoids (Hymenoptera, Scelionidae) associated with pistachio in Iran and description of a new species: *Trissolcus darreh* Talamas. In: Lahey Z, Talamas E (Eds) Advances in the Systematics of Platygastroidea III. Journal of Hymenoptera Research 87: 291–308. https://doi.org/10.3897/jhr.87.72838

Abstract
Surveys for egg-parasitoid wasps were conducted in Rafsanjan, Iran, on two species of Pentatomidae (Hemiptera) found in pistachio orchards, *Acrosternum arabicum* Wagner and *Brachynema signatum* Jakovlev. Five species of Scelionidae (Platygastroidea) were recovered, including one that is here described as new: *Psix saccharicola* (Mani), *Trissolcus colemani* (Crawford), *T. darreh* Talamas **sp. nov.**, *T. perepelovi* (Kozlov), and *T. semistriatus* (Nees). In addition to describing a new species, we report new host associations, provide COI barcodes for four of these species, and discuss host-related intraspecific variation in *T. darreh* and *T. perepelovi*.

Keywords
Trissolcus, biological control, Platygastroidea

Introduction

Pistachio nuts, *Pistacia vera* L., comprise one of the most important and valuable crops cultivated in Mediterranean countries (Greece, Turkey, Spain, Italy, and Tunisia), the Middle East (Syria and Iran), Australia and the southwestern United States (Arizona and California) (Kaska 1994; Sheibani 1995; Ferguson 2016). Pistachios are the major agricultural product in the tropical regions of Iran, especially in Rafsanjan, Kerman Province, which is the country's main pistachio producing area (Mehrnejad 2020). Pistachio is one of the most important export products in Iran and plays a key role in the agricultural economy. Hence, it is essential to identify factors that affect pistachio production. The activity of various pests is an important factor that can reduce yield in Iran's pistachio orchards and is much more significant than other harmful biotic factors, such as nematodes and fungal and bacterial pathogens. Many phytophagous Hemiptera in the families Pentatomidae, Miridae and Lygaeidae are considered worldwide pistachio pests and can cause remarkable damage to the fruits during the growing season (Mehrnejad 2020). Based on previous studies, pentatomid stink bugs are a key pest group and ranked as the second most important pests in pistachio orchards (Mehrnejad et al. 2013).

The damage of stink bugs according to the pistachio fruit phenology is divided into two stages. The first, epicarp lesion, occurs early in the season when the nuts are small, prior to shell hardening. The second, kernel necrosis, occurs during kernel development between complete shell hardening and complete ripening of the kernel. At this stage, stink bugs act as the vector of *Nematospora coryli* Kurtzman (Saccharomycetales: Saccharomycetaceae), the causal agent of stigmatomycosis which can cause serious damage to the pistachio yield during outbreaks of pentatomid bug populations (Michailides et al. 1987; Daane et al. 2005, 2016; Mehrnejad 2014). Various pentatomid bug species are known from pistachio orchards such as *Acrosternum breviceps* (Jakovlev), *Acrosternum arabicum* Wagner, *Brachynema germari* Kolenati, *Carpocoris coreanus* Distant, *Chroantha ornatula* (Herrich-Schäffer), and *Dolycoris baccarum* (Linnaeus) (Mehrnejad 2001, 2013a, b; Mehrnejad et al. 2013). Other species, including, *Acrosternum millieri* (Mulsant and Rey), *Apodiphus amygdali* (Germar), *Acrosternum heegeri* Fieber and *Brachynema signatum* Jakovlev were reported as major pentatomid bugs from pistachio regions in the 1970s (Ershad and Barkhordary 1974a-b, 1976; Samet and Akbary 1974). Currently, *B. germari* and *A. arabicum* are the most abundant pentatomid species in Iranian pistachio orchards (Mehrnejad 2020).

Parasitoids are the most dominant natural enemies due to their high rates of parasitism and diversity and have great potential for control of pentatomid populations (Mehrnejad 2013b; Mehrnejad 2020). Based on available information, natural regulation of stink bug populations in pistachio orchards is mostly from egg-parasitoid wasps in the families Scelionidae and Encyrtidae where the rate of egg parasitism can reach 95% (Mernejad 2013b). Within this parasitoid complex, species of *Trissolcus* Ashmead (Scelionidae) have the greatest diversity and a wide distribution in Iranian pistachio plantations (Mehrnejad 2013b, 2014; Mohammadpour et al. 2016; Tavanpour et al. 2017).

The goal of this study is to investigate the scelionid fauna associated with stink bug eggs in pistachio orchards and better support future control of these pests. Although not the first such study, it is the first since Palearctic *Trissolcus* was revised by Talamas et al. (2017) with subsequent refinement by Tortorici et al. (2019). The identification tools provided by these publications enable us to determine species with greater accuracy and provide a more nuanced analysis of new morphological and molecular data.

Materials and methods

Colonies of *Acrosternum arabicum* and *Brachynema signatum*

The initial populations of *Acrosternum arabicum* and *Brachynema signatum* (adults and eggs) were collected from pistachio plantation areas around Rafsanjan (30°42'2" N and 55°53'51"E) (2016–2018) and transferred to a climate-controlled room (27±1°C, L:D 16:8, and 65±5% RH). The stink bugs were kept in ventilated plastic boxes (13 × 20 × 30 cm) and were reared on an alternative diet, *Phaseolus vulgaris* L. (pods of green bean) for *A. arabicum* and *Kali turgidum* (Dumort.) Guterm. (Amaranthaceae), a common weed in pistachio orchards, for *B. signatum*. Female adult individuals were provided with paper towels as ovipositional substrates. Plastic boxes were checked daily, and egg masses were collected and used to maintain the colony and for collecting and rearing egg parasitoids. Furthermore, every two days, the boxes were cleaned and food was replaced (Mohammadpour et al. 2016).

Colony of parasitoid species

Sentinel egg masses were used to collect parasitoid wasps. For this purpose, more than 50 egg masses of *A. arabicum* and *B. signatum* (<1 h old) were glued on yellow cards (7 × 7 cm) then were attached at different heights in pistachio trees in various locations in the orchard (Mohammadpour et al 2016). Sentinel egg cards were collected every 3 days and parasitized eggs, identified by their darker color,were kept in a climate chamber (27±1°C, L:D 16:8, and 65±5% RH, EGCS 190 HR 3S, Equitec, Madrid, Spain) until adult parasitoids emerged. In order to have sufficient numbers for molecular and morphological identification, mated adult females of each species were placed in plastic Falcon tubes (15 ml) and provided with 10% honey and water mixture and fresh egg masses for 24 h. Centrifuge tubes containing parasitized eggs were then transferred to the growth chamber under above mentioned conditions for the incubation period.

Taxonomic analysis and identification

DNA extraction, PCR and sequencing were conducted at the Florida State Collection of Arthropods, Gainesville, Florida, USA, as outlined in Ganjisaffar et al. (2020), using the primers of Folmer et al. (1994). For samples that did not produce a visible PCR product, subsequent attempts were made to amplify COI using the primer pairs listed in Talamas et al. (2021). Brightfield images were produced with a Macropod imaging system using a 20X objective lens and rendered in Helicon Focus. The data and images associated with specimens from this study are deposited in the database of the Museum of Biological Diversity of The Ohio State University and can be retrieved by entering the collecting unit identifier (CUID) for each specimen at mbd-db.osu.edu (Table 2). All specimens are deposited in the Florida State Collection of Arthropods (FSCA), Gainesville, Florida, USA. Specimens were identified using the keys of Johnson and Masner (1985), Talamas et al. (2017) and Tortorici et al. (2019).

Character annotations

eps episternal foveae (Figures 6, 9, 14)
hoc hyperoccipital carina (Figure 10)
mshs mesoscutal humeral sulcus (Figure 7)
nes netrion sulcus (Figure 6)
of orbital furrow (Figures 10, 14)

Results

COI barcoding

The COI barcoding region was amplified and sequenced from three parasitoid species retrieved in this study (Table 1.)

Psix saccharicola (Mani)

Identification. *Psix saccharicola* was identified by the dark brown radicle and more brightly colored scape, metascutellum (dorsellum) with ventral lip smooth, frons without submedian carina, apex of T2 smooth, acetabular field glabrous, and S2 sulci nearly continuous posteriorly.

Material examined. Rafsanjan, Kerman Prov., Iran, 2019, reared from eggs of *Acrosternum arabicum*, 15 females, 14 males: FSCA 00093758, 00093769, 00094277, 00094284, 00094301, 00094311, 00094316, 00094323, 00094326, 00094330, 00094343, 00094347, 00094354, 00094362, 00094367, 00094374–00094375, 00094384, 00094386, 00094407, 00094423, 00094433, 00094450, 00094454, 00094458, 00094886, 00095707–00095708; DPI_FSCA 00009835.

Comments. *Psix saccharicola* has also been reported to parasitize the eggs of *Acrosternum breviceps* and *Brachynema germari* (Mohammadpour et al. 2016).

Figures 1–3. *Psix saccharicola* (FSCA 00094886) **1** head, anterior view **2** head and mesosoma, lateral view **3** head, mesosoma, metasoma, dorsolateral view.

Figure 4. *Psix saccharicola* (FSCA 00094886), head, mesosoma, metasoma, ventral view.

Table 1. Results of COI barcoding.

Species	Collecting Unit Identifier (CUID)	Genbank accession
Psix saccharicola	DPI_FSCA 00009835	MZ715050
	FSCA 00095707	MZ715051
	FSCA 00095708	MZ715052
Trissolcus darreh	FSCA 00090925	Suppl. material 1
Trissolcus semistriatus	DPI_FSCA 00009834	MZ715053
Trissolcus perepelovi	DPI_FSCA 00009837	MZ715054
	FSCA 00094844	MZ715055

Table 2. List of specimens photographed. Full resolution images are deposited at mbd-db.osu.edu and can be retrieved via the CUID.

Species	CUID
Psix saccharicola	FSCA 00094886
Trissolcus colemani	FSCA 00093792
	FSCA 00094244
Trissolcus darreh	FSCA 00090925
	FSCA 00094267
	FSCA 00094878
	FSCA 00095713
Trissolcus perepelovi	FSCA 00094875
	FSCA 00093812
	FSCA 00094223
Trissolcus semistriatus	FSCA 00094876

Trissolcus colemani (Crawford)

Identification. *Trissolcus colemani* was identified using characters presented in Tortorici et al. (2019) which include a complete netrion sulcus, a foveate mesoscutal humeral sulcus, the presence of episternal foveae, and the first laterotergite without setae.

Material examined. Rafsanjan, Kerman Prov., Iran, 2019, reared from eggs of *Brachynema signatum*; 6 females: FSCA 00093792, 00093789, 00093821, 00094241, 00094244, 00094260.

Comments. Tortorici et al. (2019) reported multiple host associations for *T. colemani*, including *B. germari*. To our knowledge, this is the first report of *T. colemani* parasitizing eggs of *B. signatum*.

Trissolcus darreh Talamas, sp. nov.

http://zoobank.org/FDF519D3-954E-40ED-A871-CFFCED74B8A9

Description. Female body length: 0.93–1.17 mm (n = 24). Male body length: 0.92–1.02 mm (n = 6).

Antenna. Color of radicle: yellow. Length of radicle: less than width of clypeus. Color of A1–A6 in female: variably yellow to brown. Color of A7–A11 in female: brown to black. Claval formula: 1-2-2-2-2.

Figure 5. *Trissolcus colemani* (FSCA 00094244), lateral habitus.

Figures 6–7. *Trissolcus colemani* **6** female (FSCA 00093972), mesosoma, ventrolateral view **7** female (FSCA 00094244), mesosoma, dorsolateral view.

Figure 8. *Trissolcus darreh*, holotype female (FSCA 00095713), habitus, anterolatereal view.

Head. Facial striae: absent. Number of clypeal setae: 2. Shape of gena in lateral view: narrow. Genal carina: absent. Malar striae: absent. Sculpture of malar sulcus: unknown. Orbital furrow: constricted or poorly defined ventrally. Macrosculpture directly dorsal to the antennal scrobe: absent. Preocellar pit: present. Setation of lateral frons: moderately dense. Punctation of lateral frons: absent. Sculpture directly ventral to preocellar pit: smooth. Rugae on lateral frons: absent. OOL: less than one ocellar diameter. Hyperoccipital carina: present, weakened medially. Macrosculpture of posterior vertex: absent. Microsculpture on posterior vertex along occipital carina: coriaceous. Anterior margin of occipital carina: crenulate. Medial part of occipital carina in dorsal view: rounded.

Mesosoma. Epomial carina: present. Macrosculpture of lateral pronotum directly anterior to netrion: finely rugulose. Netrion sulcus: incomplete, not well-defined dorsally. Pronotal suprahumeral sulcus in posterior half of pronotum: undifferentiated from sculpture of dorsal pronotum. Number of episternal foveae: 0; 1; 2. Course of episternal foveae ventrally: distinctly separate from postacetabular sulcus. Course of episternal foveae dorsally: distinctly separate from mesopleural pit. Subacropleural sulcus: present. Speculum: transversely strigose; smooth. Mesopleural pit: extending ventrally into slender, shallow furrow. Mesopleural carina: absent. Sculpture of femoral depression: smooth. Patch of striae at posteroventral end of femoral depression: absent; indicated by lines of microsculpture. Setal patch at posteroventral end of femoral depression: present as a line of setae. Microsculpture of anteroventral mesopleuron: present only on anterior face of mesopleuron bulge. Macrosculpture of anteroventral mesopleuron: absent. Postacetabular sulcus: comprised of small crenulae. Mesopleural epicoxal sulcus: present as a smooth furrow. Setation of posteroventral metapleuron:

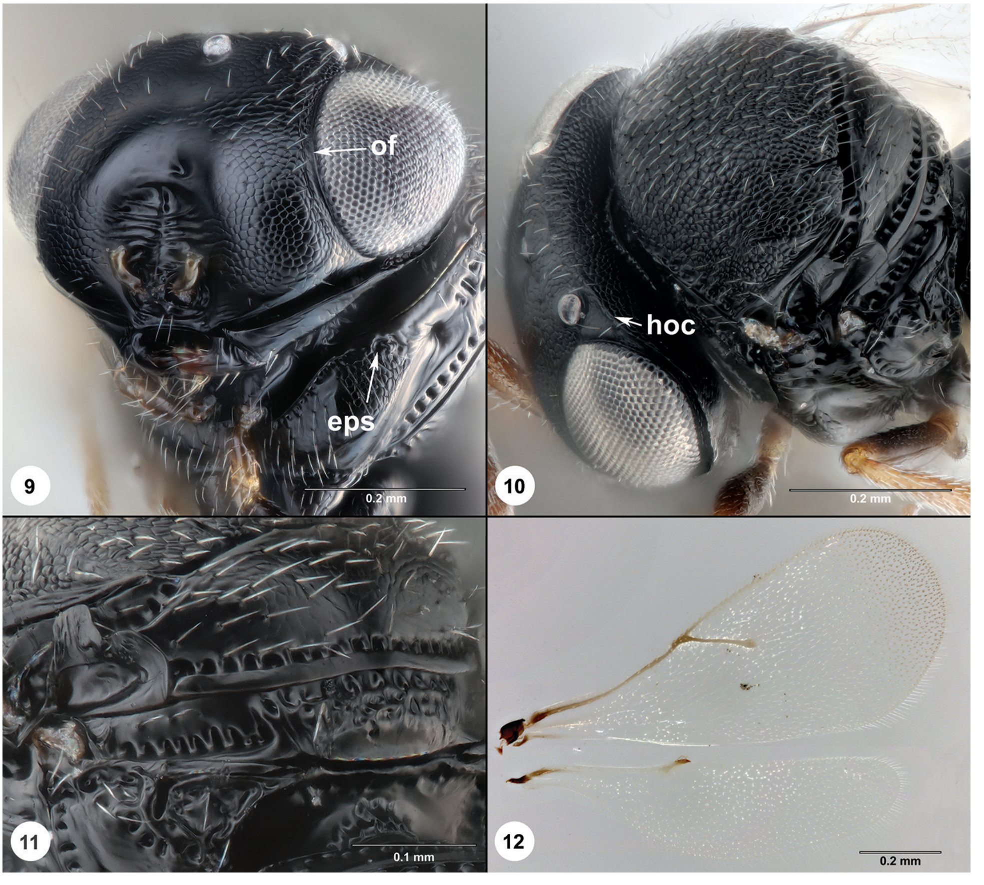

Figures 9–12. *Trissolcus darreh* **9** head and mesosoma, anterolateral view (FSCA 00090925) **10** head and mesosoma, dorsolateral view (FSCA 00094878) **11** mesosoma, posterolateral view (FSCA 00094878) **12** wings, dorsal view (FSCA 00095713).

absent. Sculpture of dorsal metapleural area: absent. Posterodorsal metapleural sulcus: present as a line of foveae. Paracoxal sulcus in ventral half of metapleuron: absent. Length of anteroventral extension of metapleuron: short, not extending to base of mesocoxa. Apex of anteroventral extension of metapleuron: acute. Metapleural epicoxal sulcus: present as coarse rugae. Mesoscutal humeral sulcus: present as a simple furrow. Median mesoscutal carina: absent. Microsculpture of mesoscutum: granular throughout. Mesoscutal suprahumeral sulcus: comprised of foveae. Length of mesoscutal suprahumeral sulcus: two-thirds the length of anterolateral edge of mesoscutum. Parapsidal line: present. Notaulus: present. Median protuberance on anterior margin of mesoscutellum: absent. Shape of dorsal margin of anterior lobe of axillar crescent: unknown. Sculpture of anterior lobe of axillar crescent: dorsoventrally strigose. Area bound by axillar crescent: smooth. Macrosculpture of mesoscutellum: absent. Microsculpture on mesoscutellum: unknown. Median mesoscutellar carina: absent. Seta-

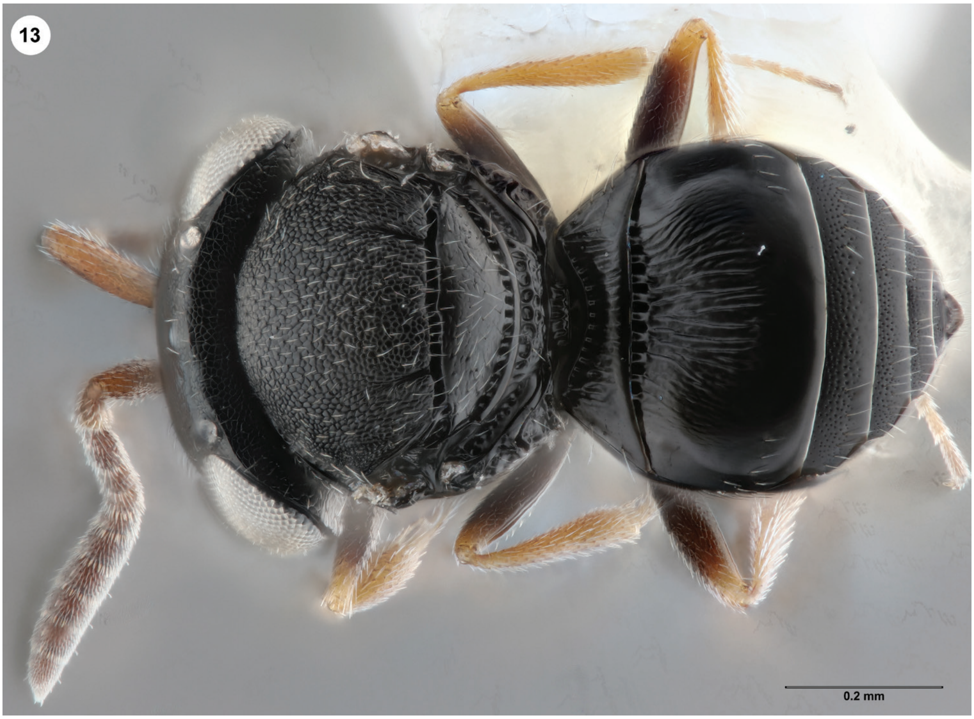

Figure 13. *Trissolcus darreh*, habitus, dorsal view (FSCA 00094878).

tion of posterior scutellar sulcus: present. Form of metascutellum: single row of foveae along anterior margin, rugulose posteriorly. Metanotal trough: foveate, foveae occupying less than half of metanotal height. Metapostnotum: invaginated near lateral edge of metascutellum. Anteromedial portion of metasomal depression: smooth.

Wings. Length of postmarginal vein: about 1.5 times as long as stigmal vein. Color of setae on fore wing: white throughout, brown at distal end.

Legs. Color of legs: coxae and femora dark brown to black, otherwise pale brown to yellow. Anteroventral area of hind femora: not covered by setae.

Metasoma. Width of metasoma: about equal to width of mesosoma. Number of sublateral setae (on one side): 0. Setation of laterotergite 1: absent. Length of striation on T2: extending two-thirds the length of the tergite. Setation of T2: present only in posterolateral corner. Setation of laterotergite 2: present.

Material examined. Rafsanjan, Kerman Prov., Iran, 2019; Holotype female (FSCA 00095713, deposited in FSCA) reared from eggs of *Acrosternum arabicum*; Paratypes: 32 females, 6 males: FSCA 00090925, 00093783–00093784, 00093788, 00093793, 00093798, 00093805, 00093832, 00093842, 00093845, 00093854, 00094227–00094228, 00094230–00094232, 00094235–00094236, 00094238–00094240, 00094242, 00094246–00094247, 00094254–00094255, 00094265, 00094267, 00094269, 00094275, 00094878, 00095711–00095712, 00095760 reared from eggs of *Acrosternum arabicum*; FSCA 00094248, 00094273, 00095759 reared from eggs of *Brachynema signatum*.

Figure 14. *Trissolcus darreh*, male (FSCA 00094267), head and mesosoma, ventrolateral view.

Intraspecific variation. In the specimens reared from *B. signatum*, the mesopleuron directly ventral to the femoral depression projects more sharply than in the specimens reared from *A. arabicum*. However, because we have only three females and one male reared from *B. signatum*, more specimens are needed to confirm that this difference is host related. Other characters with notable variation are the orbital furrow, the hyperoccipital carina, the color of setae on the fore wing and subtle differences in the episternal foveae. In females, the orbital furrow tends to become constricted ventrally, but in some specimens the medial edge of the furrow is not defined where it intersects the malar sulcus. This condition was typical for the small number of males that we examined. The hyperoccipital carina is medially weakened in all specimens and in some it is essentially absent between the lateral ocelli. Variation in the color of the wing setae can be difficult to assess without slide-mounting the wings because the perception of the color is influenced by what is behind the wing, and the color difference is subtle. However, it should still be noted that setae at the apex of the fore wing appear to vary from pale to medium brown. The episternal foveae in *T. darreh* are shallow and may be irregular in shape. In most specimens, there is a single fovea, but occasionally there are two. Rarely, and usually in males, no foveae are visible.

Comments. *Trissolcus darreh* arrives at couplet 16 in the key to *Trissolcus* species of the Palearctic region by Talamas et al. (2017), where it matches neither of the leads, having neither a continuous line of episternal foveae between the postacetabular sulcus and mesopleural pit, nor abbreviated notauli. It is similar to *Trissolcus saakowi*, which has been recorded from Iran, but these species can be separated by the setation of the first laterotergite: present in *T. saakowi* and absent in *T. darreh*. *Trissolcus darreh* is also similar to *T. tumidus*, with which it shares the medially weakened hyperoccipital carina and the reduced episternal foveae. However, these two species are easily separated by the orbital furrow, being well defined at the intersection with the malar sulcus in *T. tumidus*, and the form of the mesoscutal humeral sulcus, which is a smooth furrow in *T. darreh* and is comprised of foveae in *T. tumidus*.

COI barcoding. Multiple attempts were made to amplify COI from specimens of *T. darreh* and from one specimen we were able to produce a faint band with LepF1/LepR1 primers. Sequencing produced a quality read in only in the forward direction, precluding us from uploading it to GenBank, which requires bidirectional sequencing. This sequence is unique in BOLD and GenBank. The closest match in GenBank is to *Trissolcus euschisti* (Ashmead) (MG939339.1, 84% sequence identity). In BOLD, the best matches are all ~89.5% to BINs BOLD:AAZ3289 (*Telenomus* Haliday), BOLD:ACB8142 (*Trissolcus*), and BOLD:ACB8142 (*Phanuromyia* Dodd). Identification of the latter two BINs was made based on images provided in BOLD. A FASTA file of this sequence is provided in Suppl. material 1.

Etymology. This species is given the name "darreh," a Farsi word for valley, because the form of the orbital furrow is one of its diagnostic characters.

Trissolcus perepelovi (Kozlov)

Identification. *Trissolcus perepelovi* was identified using the key of Talamas et al. (2017). Key characters used to identify this species are the absence of a hyperoccipital carina, metapleuron without setation, absence of episternal foveae, female antenna with five clavomeres, and a bulging anteroventral portion of the mesopleuron.

Material examined. Rafsanjan, Kerman Prov., Iran, 2019, reared from eggs of *Acrosternum arabicum* and *Brachynema signatum*, 85 females, 41 males: FSCA 00093760–00093762, 00093764, 00093773–00093774, 00093776–00093777, 00093779, 00093781–00093782, 00093785, 00093787, 00093791, 00093794–00093797, 00093799–00093804, 00093807–00093812, 00093814–00093815, 00093817, 00093819–00093820, 00093822–00093823, 00093825–00093831, 00093834–00093841, 00093843–00093844, 00093846–00093848, 00093850–00093853, 00093855–00093857, 00093859–00093860, 00094200–00094201, 00094203, 00094206, 00094208, 00094210, 00094212–00094214, 00094216–00094218, 00094220–00094226, 00094229, 00094233–00094234, 00094245, 00094250–00094253, 00094256–00094259, 00094262–00094264, 00094268, 00094270–00094272, 00094274, 00094276, 00094278–00094279, 00094282–00094283, 00094286–00094288, 00094291, 00094294–00094295, 00094299–00094300, 00094411, 00094875, 00095709–00095710.

Intraspecific variation. Among the specimens analyzed here, we found that there is more variation in the microsculpture of the frons (Figures 15–16) than was documented by Talamas et al. (2017). Specimens reared from *B. signatum* tend to have more micro-

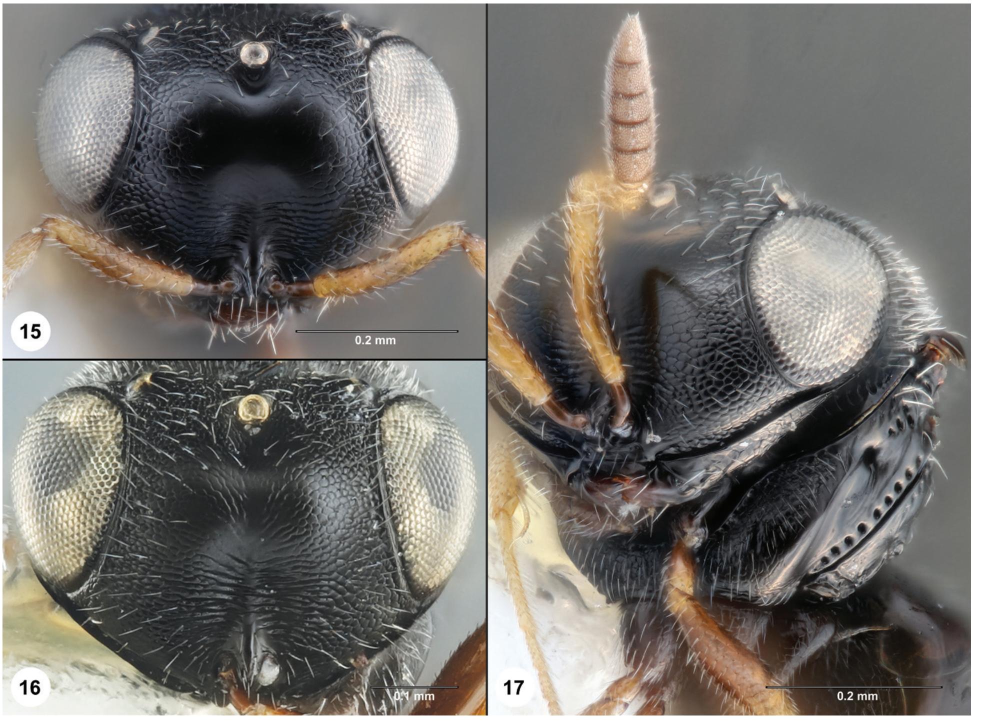

Figures 15–17. *Trissolcus perepelovi* **15** female (FSCA 00094875, ex. *A. arabicum*), head, anterior view **16** female (FSCA 00093812), head, anterior view **17** female (FSCA 00094875), head and mesosoma, ventrolateral view.

sculpture than those from *A. arabicum*, but this is not a perfect correlation. Specimens reared from *B. signatum* tend to have a metasoma that is lighter in color than those reared from *A. arabicum*, a phenomenon that Ganjisaffar et al. (2020) reported to be host related in some Nearctic *Trissolcus* species. We generated two COI barcode sequences for *T. perepelovi*, one from a specimen reared from *A. arabicum*, and the other from *B. signatum*, which have a 99.53% sequence identity. These specimens have slight variation in the degree of microsculpture on the frons and both have a dark metasoma. This suggests that the variation described above is not entirely attributable to the host species.

Comment. In this study, *T. perepelovi* was reared from the eggs of *Acrosternum arabicum* and *Brachynema germari*. It was previously reported by Mohammadpour et al. (2016), as *T. deserticola*, to parasitize the eggs of *B. germani* in Kerman province.

Trissolcus semistriatus (Nees von Esenbeck)

Identification. *Trissolcus semistriatus* was identified using diagnostic characters presented in Tortorici et al. (2019): the absence of a hyperoccipital carina, metapleuron

Figures 18–19. *Trissolcus perepelovi*, female (FSCA 00094875) **18** habitus, lateral view **19** head, mesosoma, metasoma, lateral view.

Figure 20. *Trissolcus semistriatus*, female (FSCA 00094876), habitus, lateral view.

without setation, female antenna with five clavomeres, the presence of episternal foveae, a mesoscutal humeral sulcus that is a smooth furrow, and the absence of setae on the first laterotergite. The CO1 barcode sequence from an Iranian specimen (DPI_FSCA 00009834) was found to have the best match (99.53% sequence identity) to *T. semistriatus* from the Republic of Georgia when compared to other sequences in GenBank using BLAST.

Material examined. Rafsanjan, Kerman Prov., Iran, 2019, reared from eggs of *Acrosternum arabicum*, 13 females, 13 males: DPI_FSCA 00009834; FSCA 00093757, 00093759, 00093763, 00093765–00093768, 00093770–00093772, 00093775, 00093778, 00093780, 00094280–00094281, 00094285, 00094289–00094290, 00094292–00094293, 00094296–00094298, 00094302, 00094876.

Discussion

This study is the first to document scelionid parasitoids associated with stink bug eggs in pistachio orchards since the taxonomy of Palearctic *Trissolcus* was treated by Talamas et al. (2017) and Tortorici et al. (2019). Combined with the molecular studies of Tortorici et al. (2019) and Talamas et al. (2019), these have provided a more reliable means of identifying species and highlight the necessity of systematics for biological control efforts. For example, Mohammadpour et al. (2016) and Mehrnejad (2013) reported associations between stink bugs in Iran and some *Trissolcus* species, some of which are now treated as junior synonyms (Table 3). Examination of voucher specimens from these studies will be needed to verify their determinations because the identification tools available at the time of these studies were insufficient to resolve many species of *Trissolcus*.

Given the amount of attention that Palearctic *Trissolcus* has received during recent years, it is somewhat surprising that the region contains a previously undescribed species. This discovery emphasizes the importance of continuous collaboration between those conducting field and laboratory studies, as each provides the other with the necessary specimens and data to maximize effectiveness.

Table 3. Names of *Trissolcus* species used on previous studies and their current status.

Names used in Mohammadpour et al. (2016) and Mehrnejad (2013)	Valid name	Most recent taxonomic treatment
T. agriope (Kozlov & Lê)	*T. agriope* (Kozlov & Lê)	Kozlov and Kononova (1983)
T. delucchii Kozlov	*T. tumidus* (Mayr)	Talamas et al. (2017)
T. deserticola (Kozlov)	*T. perepelovi* (Kozlov)	Talamas et al. (2017)
T. mitsukurii (Ashmead)	*T. mitsukurii* (Ashmead)	Talamas et al. (2017)
T. niceppe (Kozlov & Lê)	*T. oobius* (Kozlov)	Talamas et al. (2017)
T. oobius (Kozlov)	*T. oobius* (Kozlov)	Talamas et al. (2017)
T. semistriatus (Nees)	*T. semistriatus* (Nees)	Tortorici et al. (2019)
T. volgensis (Viktorov)	*T. scutellaris* (Thomson)	Talamas et al. (2017)

Acknowledgments

We are grateful to Vali-e-Asr University of Rafsanjan, Iran, for financial support to Fateme Ranjbar (PhD student no. 95368001). Elijah Talamas was supported by the Florida Department of Agriculture and Consumer Services-Division of Plant Industry (FDACS-DPI). We are grateful to Jonathan Bremer, Matthew Moore, Cheryl Roberts, and Lynn Combee (FDACS-DPI) for contributing images and generating molecular data.

References

Daane K, Yokota G, Krugner R, Steffan S, Da Silva P, Beede RH, Bentley WJ, Weinberger GB (2005) Large bugs damage pistachio nuts most severely during midseason. California Agriculture 59: 95–102. https://doi.org/10.3733/ca.v059n02p95

Ershad D, Barkhordary M (1974a) Host range and vectors of *Nematospora coryli* Peglion in Kerman of Iran. Iranian Journal of Plant Pathology 10: 34–39.

Ershad D, Barkhordary M (1974b) Study of three fungi causing stigmatomycosis in Iran. Iranian Journal of Plant Pathology 10: 1–8.

Ershad D, Barkhordary M (1976) Investigations on stigmatomycosis (massu disease) of pistachio. Iranian journal of Plant Pathology 12: 17–23.

Ferguson L, Kallsen CE (2016) The pistachio tree: physiology and botany. Pistachio production manual, publication, 3545, 19–26.

Folmer O, Black M, Hoeh W, Lutz R, Vrijenhoek R (1994) DNA primers for amplification of mitochondrial Cytochrome C oxidase subunit I from diverse metazoan invertebrates. Molecular Marine Biology and Biotechnology 3: 294–299.

Ganjisaffar F, Talamas EJ, Bon M-C, Perring TM (2020) First report and integrated analysis of two native *Trissolcus* species utilizing *Bagrada hilaris* eggs in California. Journal of Hymenoptera Research 80: 49–70. https://doi.org/10.3897/jhr.80.57024

Johnson NF, Masner L (1985) Revision of the genus *Psix* Kozlov & Lê. Systematic Entomology 10: 33–58. https://doi.org/10.1111/j.1365-3113.1985.tb00562.x

Kaska N (1994). Pistachio nut growing in Turkey. In I International Symposium on Pistachio 419: 161–164. https://doi.org/10.17660/ActaHortic.1995.419.26

Michailides TJ, Rice RE, Ogawa J M (1987) Succession and significance of several hemipterans attacking a pistachio orchard. Journal of Economic Entomology 80: 398–406. https://doi.org/10.1093/jee/80.2.398

Mehrnejad MR (2001) The current status of pistachio pests in Iran. Cahiers Options Méditerranéennes 56: 315–322.

Mehrnejad MR (2013a) Pest problems in pistachio producing areas of the world and their current means of control. In VI International Symposium on Almonds and Pistachios 1028: 163–169. https://doi.org/10.17660/ActaHortic.2014.1028.26

Mehrnejad MR (2013b) Abundance of parasitoids associated with two major stink bugs on pistachio trees. Applied Entomology and Phytopathology 81: 83–84.

Mehrnejad MR (2014) The pests of pistachio trees in Iran, natural enemies and control. Tehran, Sepehr publication. 272 pp. https://doi.org/10.17660/ActaHortic.2014.1028.30
Mehrnejad MR (2020) Arthropod pests of pistachios, their natural enemies and management. Plant Protection Science 56: 231–260. https://doi.org/10.17221/63/2019-PPS
Mehrnejad MR, Linnavuori RE, Alavi SH (2013) Hemipteran bugs associated with pistachio trees and notes on major species. Zoology and Ecology 23: 29–40. https://doi.org/10.1080/21658005.2013.774832
Mohammadpour M, Ziaaddini M, Jalali MA, Hashemirad H, Mohammadi-Khoramabadi, A (2016) Egg parasitoids of the pistachio green stink bug, *Brachynema germari* (Hemiptera: Pentatomidae) in Kerman province, Iran. Zoology and Ecology 26: 28–34. https://doi.org/10.1080/21658005.2015.1120544
Samet K (1974) Three injurious butterflies of pistachio trees in Kerman province. In: Proceedings of the 5th plant protection congress of Iran, Tabriz, 1974: 11–12.
Sheibani A (1995) Distribution, use and conservation of pistachio in Iran. In: Padulosi S, Caruso T, Barone E (Eds) Taxonomy, distribution, conservation and uses of *Pistacia* genetic resources, International Plant Genetic Resources Institute (IPGRI), Rome.
Tavanpour T, Mehrnejad MR, Sarafrazi A, Imani S (2017) Distribution modelling of four scelionid egg parasitoids of green stink bugs (Hemiptera: Pentatomidae). Biologia 72: 53–61. https://doi.org/10.1515/biolog-2017-0010
Talamas E, Buffington M, Hoelmer K (2017) Revision of Palearctic *Trissolcus* Ashmead (Hymenoptera: Scelionidae). In: Talamas EJ, Buffington ML (Eds) Advances in the Systematics of Platygastroidea. Journal of Hymenoptera Research 56: 3–185. https://doi.org/10.3897/jhr.56.10158
Talamas EJ, Bon M-C, Hoelmer KA, Buffington ML (2019) Molecular phylogeny of *Trissolcus* wasps (Hymenoptera, Scelionidae) associated with *Halyomorpha halys* (Hemiptera, Pentatomidae). In: Talamas E (Eds) Advances in the Systematics of Platygastroidea II. Journal of Hymenoptera Research 73: 201–217. https://doi.org/10.3897/jhr.73.39563
Talamas EJ, Bremer JS, Moore MR, Bon M-C, Lahey Z, Roberts CG, Combee LA, McGathey N, van Noort S, Timokhov AV, Hougardy E, Hogg B (2021) A maximalist approach to the systematics of a biological control agent: *Gryon aetherium* Talamas, sp. nov. (Hymenoptera, Scelionidae). In: Lahey Z, Talamas E (Eds) Advances in the Systematics of Platygastroidea III. Journal of Hymenoptera Research 87: 323–480. https://doi.org/10.3897/jhr.87.72842
Tortorici F, Talamas EJ, Moraglio ST, Pansa MG, Asadi-Farfar M, Tavella L, Caleca V (2019) A morphological, biological and molecular approach reveals four cryptic species of *Trissolcus* Ashmead (Hymenoptera, Scelionidae), egg parasitoids of Pentatomidae (Hemiptera). In: Talamas E (Eds) Advances in the Systematics of Platygastroidea II. Journal of Hymenoptera Research 73: 153–200. https://doi.org/10.3897/jhr.73.39052

Supplementary material 1

FASTA file

Authors: Fateme Ranjbar, M. Amin Jalali, Mahdi Ziaaddini, Zahra Gholamalizade, Elijah J. Talamas

Data type: molecular data

Link: https://doi.org/10.3897/jhr.87.72838.suppl1